EurJIC
European Journal of Inorganic Chemistry

A Journal of ChemPubSoc Europe

Accepted Article

Title: A Luminescent pH-Responsive Ternary Eu3+ Complex of β-diketonate and Terpyridine Derivative as Sensitizing Antenae: Photophysical Aspects, Anion Sensing and Biological Interactions

Authors: Kritika Gupta and Ashis K. Patra

To be cited as: *Eur. J. Inorg. Chem.* 10.1002/ejic.201701495

Link to VoR: http://dx.doi.org/10.1002/ejic.201701495

WILEY-VCH

10.1002/ejic.201701495

WILEY-VCH

FULL PAPER

A Luminescent pH-Responsive Ternary Eu^{3+} Complex of β-diketonate and Terpyridine Derivative as Sensitizing Antenae: Photophysical Aspects, Anion Sensing and Biological Interactions

Kritika Gupta[a] and Ashis K. Patra*[a]

Abstract: A highly luminescent stable Eu^{3+} complex, $[Eu(tta)_3(naptpy)]$ (**1**) [tta = 2-thenoyltrifluoroacetone, naptpy = 2-(4-([2,2':6',2''-terpyridin]-4'-yl)phenyl)-6-bromo-1H benzo[de]isoquinoline -1,3(2H)-dione] was designed as pH-responsive anion sensing probe. Complex **1** was synthesized and characterized using various physicochemical and spectral methods like FT-IR, ^{1}H-NMR, ESI-MS, UV-vis and emission spectral studies. A photosensitization mechanism with two antennae, viz. tta and naptpy for Eu-luminescence by energy transfer to emissive $^5D_0$ states of Eu^{3+} through corresponding excited triplet states of the ligands are shown. It displays strong luminescence properties, remarkable photostability, long luminescence lifetime (τ = 0.365 ms) in H_2O and absence of any coordinated inner-sphere water (q < 1). The pH-dependent study showed that emission intensity of **1** was quenched or 'switched off' upon displacement of the β-diketonate antenna due to the acid sensitivity of α-proton in tta and subsequent ligand exchange reaction. The anion sensitivity of the probe was evaluated using a series of anions in aqueous DMF. Upon binding to citrate, F^- and HCO_3^-, luminescence quenching of complex **1** was demonstrated, while only minor luminescence changes were observed in the presence of other anions suggesting oxophillicity or stronger binding affinity with the hard oxoanions with hard Eu^{3+} Lewis acid. The probe shows efficient DNA (K_b = 6.53 X 10^4 M^{-1}) and BSA (K_{BSA} = 5.09 X 10^5 M^{-1}) binding affinity under physiological condition. Quenching in luminescence intensity upon interaction with CT-DNA suggests possible luminescence-based sensing application.

Introduction

Recognition and sensing of different anions (e.g., F^-, CN^-, HCO_3^-, citrate, ascorbate, etc.) have aroused significant attention due to their association in various biological and metabolic processes as well as their detrimental effect on certain organisms and the environment.[1-7] Sensitive response requires specific reactive receptor composed of organic fluorophores to monitor particular anions.[3,4] Lanthanide (Ln^{3+}) complexes provide strong electrostatic interaction with such anions as they are oxophilic with higher charge density (e/r).[5] Numerous lanthanide-based luminescent sensors with high sensitivities and specificities have been reported previously.[5-7] Several multidentate cyclen-based lanthanide complexes for selective detection of various anions at Ln^{3+} centers in aqueous media were reported.[6,7] Gunnlaugsson et al. have reported a cylen based luminescent self-assembly of Eu^{3+} ternary complex and β-diketonate in water where the ternary Eu^{3+} self-assembly is highly pH dependent.[7] Further, they employed this probe as luminescent sensor for anions, where the β-diketonate antenna is displaced by anions with concomitant changes in the Eu^{3+} emission intensity.

Unique emission properties like longer excited state lifetime (τ), large ligand-induced Stokes' shift and sharp emission bands corresponds to the characteristic f→f transitions in the inner 4f shell of Ln^{3+}. These transitions are shielded from the influence of the chemical environment by the outer $5s^25p^6$ subshells which make optical properties of lanthanide complexes are rather more fascinating. The radiative transition in Ln^{3+} is parity-forbidden thus inducing only weak absorbance and ineffective direct excitation.[8] The luminescence efficiency of the Ln^{3+} complex is mainly due to its strongly absorbing ligands, that absorbs light and transfers its energy from ^3T state to the emissive excited state of the Ln^{3+} ion, which can then decay non-radiatively or emit light. This phenomenon of indirect sensitization is known as "*antenna effect*".[8,9] The fascinating luminescence and magnetic properties of lanthanides have diverse applications in bioimaging, laser source, luminescent probes, sensors, drug delivery, medical diagnosis, MRI, labels for biomolecules and stains for cellular imaging.[10-15]

We are interested in exploring such emissive lanthanide probes for sensing and recognition of bioanalytes and cellular imaging.[16,17] Herein, we have designed a luminescent Eu^{3+}-probe based on 1,8-naphthalimide appended planer terpyridine ligand (naptpy) and 2-thenoyltrifluoroacetone (tta) as photosensitizing antennae (Scheme 1). We have chosen 2-thenoyltrifluoroacetone (Htta) as β-diketonate ligand to introduce pH-sensitivity and potential anion sensing application *via* lanthanide based displacement assay. Usually, tta is highly sensitive to pH changes due to the presence of α-acidic proton. The three tta ligands provide hard oxygen donor sites which forms a thermodynamically stable Eu^{3+} complex and promote effective energy-transfer to Eu^{3+} for visible light emission by serving as ''*antenna*'' with enhancement in the Eu^{3+} luminescence.[18-20] Moreover, low energy C-F bonds helps to reduce non-radiative quenching of lanthanide excited state which consequently displays longer emissive lifetimes (τ),

[a] Department of Chemistry
Indian Institute of Technology Kanpur, Kanpur 208016
Uttar Pradesh, India
E-mail: akpatra@iitk.ac.in
https://www.iitk.ac.in/new/ashis-k-patra
Supporting information for this article are available on the WWW under http://dx.doi.org/10.1002/ejic.201701495.

enhanced quantum yield (ϕ) and higher luminescence intensity. However, often such lanthanide complexes have coordinated water molecules or labile anion or solvents which undergo undesirable inner-sphere water-exchange reactions in aqueous media, resulting non-radiative luminescence quenching *via* O-H oscillators which is detrimental for an imaging probe. A second ligand could provide a coordinatively saturated and structurally rigid Eu-complex and acts as a chromophoric antenna. This approach will ultimately avoid nonradiative luminescence quenching through vibrational energy transfer (VET) to O–H, N–H and C–H oscillators hence, enhancing desired optical properties and making them ideal as imaging probes.[17-19] The naptpy ligand provides tridentate binding site coordination for Eu^{3+}. The terpyridine (tpy) is an excellent neutral ligand for Eu^{3+}; it offers efficient sensitization of Eu^{3+} centred luminescence by reducing non-radiative decay of the excited states of the europium ion. The tpy moiety also acts as a light harvesting photosensitizing antenna, making it highly attractive for incorporation into single ligand design.[21-23] Moreover, tpy and 1,8-naphthalimide derivatives were extensively used due to their excellent fluorescence properties, photostability and effective interactions with biomolecules. The choice of naptpy as a ligand is based on the fact that tpy with 1,8-naphthalimide moiety could act as photosensitizer cum DNA binders. Moreover, the photophysical properties of naphthalic anhydride derivatives can be tuned through structural modification on either at the nitrogen of the imide site or at the aromatic 'naphthalene' moiety itself.[24] These derivatives were extensively used as strongly absorbing and colourful dyes, building block for artificial light harvesting arrays, fluorescent chemosensors for metal cations and anions in recent years.[24,25]

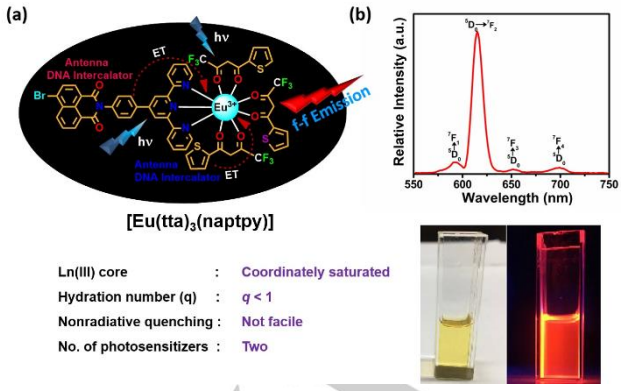

Scheme 1. (a) Design strategy for luminescent $[Eu(tta)_3(naptpy)]$ (**1**) probe highlighting various photophysical parameters. (b) Time-delayed luminescence spectra of Eu(III) complex in aq. DMF at 298 K with corresponding assignments of $^5D_0 \rightarrow {}^7F_J$ transitions [λ_{ex}= 349 nm, delay and gate time = 0.1 ms, Ex. and Em. slit width = 5 nm] (top) and photographs Eu(III) complex under ambient light and UV-light exposure (bottom).

With the aim mentioned above of pH dependent quenching process, we have developed a stable coordinatively saturated photosensitized luminescent complex, $[Eu(tta)_3(naptpy)]$ (**1**) which inhibits binding of H_2O to Ln^{3+} and prevent non-radiative quenching by vibrational energy transfer (VET) and later on can be used as a platform for sensing anions (Scheme 1). Complex **1** act as a luminescent sensor for the detection of anions such as citrate, HCO_3^- and F^-, where characteristic ($^5D_0 \rightarrow {}^7F_2$) Eu^{3+} emission was quenched or '*switched off*' upon displacing β-diketone antenna on recognition of these anions. Complex **1** also exhibit potential binding affinity with DNA and BSA in an aqueous medium due to presence of planar naptpy ligand.

Results and Discussion

Synthesis and general aspects

$[Eu(tta)_3(naptpy)]$ (**1**) was synthesized in high yield (~71%) by reacting $[Eu(tta)_3(H_2O)_2]$ with naptpy in THF (Scheme 2). The naptpy ligand and the complex **1** were fully characterized by ^{1}H-NMR, ESI-MS, FT-IR, Job's plot and UV-Vis spectroscopy. The complex **1** was stable under ambient condition. The ESI-MS analysis of complex **1** in DMF showed respective molecular ion peak as $[\mathbf{1}\text{-tta}]^+$ with calculated isotopic distribution exhibiting it's structural integrity in solution (Fig. S2, SI). The FT-IR spectra shows $\nu_{C=O}$ at 1640 cm^{-1} of Htta shifted to 1611 cm^{-1} for complex **1** indicating strong interaction between the oxygen atoms from Htta and Eu^{3+}, $\nu_{C=N}$ at 1423 cm^{-1} for complex **1** also shifted to lower energy compared to the naptpy ligand at 1585 cm^{-1} suggesting possible coordination through *N,N,N*-donor naptpy ligand to Ln^{3+}. The presence of ν_{Ln-O} and ν_{Ln-N} vibrations also confirms such coordination mode. A strong band at 1134 cm^{-1} assigned to C-F stretching mode of CF_3 (Table 1).

Table 1. Selected FT-IR frequencies ($\bar{\nu}$ / cm^{-1}, in KBr disc) and their assignments for free naptpy, $[Eu(tta)_3(naptpy)]$ (**1**) and Htta

($\bar{\nu}$ in cm^{-1})	$[Eu(tta)_3(naptpy)]$ (**1**)	naptpy	Htta
ν (C=O)	1611	-	1640
ν (C=N)	1423	1585	-
ν (C-N)	1184	1223	-
ν (C-F)	1134	-	1111
ν (Eu-O)	458	-	
ν (Eu-N)	518	-	-

The UV-visible spectra of **1** in 5mM Tris-buffer showed two major ligand based π-π^* ($S_0 \rightarrow S_1$) transitions ranging from ~260 to 400 nm. The absorption maxima at 339 nm for free Htta ligand were blue-shifted to 349 nm in complex **1** due to electronic perturbation induced by the coordinated Eu^{3+} (Fig. 1a). The emissive nature of complex **1** was also probed using fluorescence spectroscopy that revealed a broad band ~350-550 nm due to the ligand-centred emission possibly due to the ligand based π–π^* excited state (Fig. 1b).

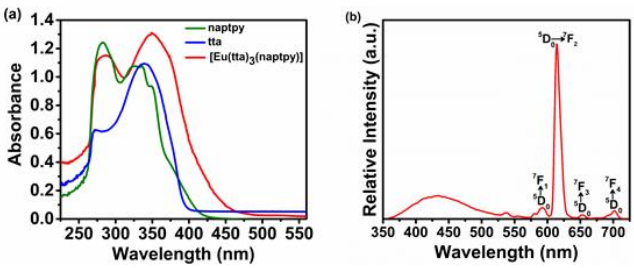

Figure 1. (a) UV-visible absorption spectral traces of complex **1**, tta and naptpy ligands in 5 mM Tris-buffer (with 2% DMF) at pH 7.2 (T = 298 K), [**1**] = 10 μM. (b) Steady state emission spectra for complex **1** recorded in fluorescence in 5

mM Tris-buffer (with 2% DMF) (T = 298 K). λ_{ex} = 349 nm, Ex. and Em. slit width = 5 nm.

The Job's plot analysis and luminescence titrations were performed to evaluate the stoichiometry between Eu^{3+} and the respective ligands and speciation of complex **1** in aqueous solution at pH 7.2. As shown in Fig. 2a, the Job's plot exhibited maxima at 0.5 mole fraction, indicating 1:1 stoichiometry of $[Eu(tta)_3(H_2O)_2]$ and naptpy. Subsequently, the binding stoichiometry between tta and Eu^{3+} was also evaluated (Fig. S3, SI). The Job's plot displayed a maximum at 0.75 molar fraction, indicating 1:3 stoichiometry between Eu^{3+} and tta. Moreover, the naptpy to $[Eu(tta)_3(H_2O)_2]$ ratio was also calculated by luminescence titrations of naptpy (10 μM) with varying concentration of $[Eu(tta)_3(H_2O)_2]$ in 5 mM Tris-buffer at pH 7.2. The resulting titration curve exhibit best fitting with a 1:1 stoichiometry (Fig. 2b). These results unambiguously proved that $[Eu(tta)_3(naptpy)]$ as the sole major species in aqueous solution at physiological pH.

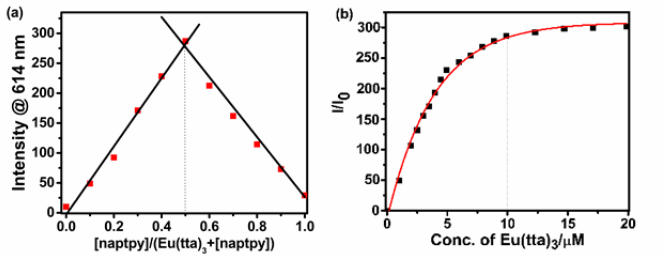

Figure 2. (a) Job's plot of the reaction between $[Eu(tta)_3(H_2O)_2]$ and naptpy in 5 mM Tris-buffer (pH 7.2) (the total concentration of $[Eu(tta)_3(H_2O)_2]$ and naptpy was kept at 20 μM). (b) Luminescence titration of naptpy with varying concentration of $[Eu(tta)_3(H_2O)_2]$ in 5 mM Tris-buffer at pH 7.2. The resulting luminescence titration curve was analyzed by a non-linear regression based on a 1:1 binding isotherm model (T = 298 K, λ_{ex} = 349 nm, λ_{em} = 614 nm, Ex. and Em. slit width = 5 nm).

Time-dependent absorption spectra of **1** in 5 mM Tris-buffer was recorded for 4 h at 298 K do not show any observable changes suggesting it's appreciable stability in solution and unlikely any ligand-exchange reactions occurring at neutral pH. Further, emission/luminescence spectra were also recorded at regular time interval upon irradiation with complex **1** (Fig. S5, SI). The steady-state fluorescence and luminescence intensity of complex **1** show no notable changes (only ~8% reduction) in its luminescence intensity. These observations strongly indicate remarkable photostability of complex **1** in solution (Fig. S5, SI).

Photophysical Properties

Lanthanide complexes are well-known for their intense luminescence based applications ranging from biomedical imaging to sensing anions and bioanalytes based on their narrow emission bands, large Stokes' shift and long-lived excited state lifetimes (μs-ms).[26,27] The detailed photophysical studies were performed for complex **1** as discussed here.

(a) Energy Transfer Mechanism. The energy transfer pathway in luminescent Eu^{3+}-complex comprise of photoexcitation of the ligand energy to the Eu^{3+} through their corresponding triplet (T_1) states *via* intersystem crossing (ISC); finally, the Eu^{3+} ion emits when the electronic transition from $^5D_0$ to ^7F_J ground state occurs (Fig. 3).[28] Ideally, the ^3T level of ligands should be higher than the $^5D_0$ level of Eu^{3+} (17,200 cm^{-1}) for effective energy transfer (ET) and hydration number, q = 0. Moreover, the difference of optimal energy gap (ΔE) between the ligand ^3T states to the emissive excited state of Eu^{3+} ($^5D_0$) ideally should ~2500–3000 cm^{-1}.[28,29] Time-delayed luminescence spectra of $[Eu(tta)_3(naptpy)]$ (**1**) shows characteristic europium based red luminescence at λ_{ex} = 349 nm attributed to the $^5D_0 \rightarrow {}^7F_J$ f–f transitions of Eu^{3+} (J = 0-4). The most intense band at 614 nm originated from electric dipole (ED) induced hypersensitive $^5D_0 \rightarrow {}^7F_2$ transition.[30,31]

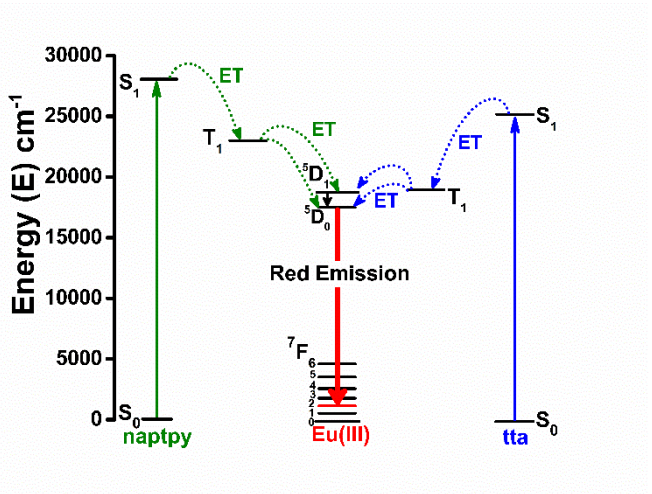

Figure 3. Schematic energy transfer diagram for $[Eu(tta)_3(naptpy)]$ (**1**) from tta and naptpy ligands (⇢ is non-radiative transition, → is radiative transition, S = singlet, T = triplet, ET = energy transfer).

The electronic energy levels of tta were at 25,164 cm^{-1} (S_1) and 18,954 cm^{-1} (T_1).[28] Density functional theory (DFT) was applied to the naptpy ligand for calculating it's energy levels which justifies the plausible energy transfer mechanism from corresponding ligand to Eu^{3+}.[32] The calculated singlet (S_1) and triplet (T_1) energy levels of the naptpy by DFT and TD-DFT analysis were located at 28,025 cm^{-1} (3.48 eV) and 22,987 cm^{-1} (2.85 eV), as schematically shown in Fig. 3. Both ligands thereby can effectively transfer the energy from their ^3T states to the $^5D_0$ state of the Eu^{3+}.[33] Therefore, in luminescent $[Eu(tta)_3(naptpy)]$, the ET-process is more facile from dual antennae to Eu^{3+} because of efficient intersystem crossing (ISC) and optimal energy gap from ligand triplet states to $^5D_0$ excited state of Eu^{3+}. The effective sensitization effect of ancillary ligand 'naptpy' on Eu^{3+} emission can also be seen on luminescence spectra of $[Eu(tta)_3.2H_2O)]$ which increases upon the addition of naptpy. Moreover, we also observed enhancement of luminescence spectra of $[Eu(naptpy)(NO_3)_3]$ upon gradual increment of 'tta'. These results further underscores the effect of sensitization by both the ligands in complex **1** (Fig. S4, SI).

(b) Photoluminescence excited state lifetimes and effect of solvents. The excited state lifetime of complex **1** was measured at 298 K by monitoring the most intense emission line ($^5D_0 \rightarrow {}^7F_2$) at λ_{em} = 614 nm under excitation at λ_{ex} = 349 nm (Fig. 4a, Table 2). The exhibited monoexponential decay is indicative of the presence of a single chemical environment around the Eu^{3+} ion. The measured data were fitted with single exponential functions given by the equation: $\boldsymbol{I(t) = I_0 + A_1 exp\ \frac{-t}{\tau}}$, where A_1 is the scalar quantity obtained from the curve fitting, I_0 = 0 is the offset value, t is the time in ms and t is the decay time for the exponential component.[34] The effect of solvent types on the emissive lifetime were studied using a variety of solvents (Table 2 and Fig. S6, SI). The lifetimes decreased in the order of $CHCl_3$ > DCM > THF > DMF > H_2O. Overall, the primary process that quenches the $^5D_0$ excited state of Eu^{3+} in solution is non-radiative relaxation via a vibronic coupling.[34-36] Presence of C-H, N-H, and O-H groups from solvents in close vicinity to the central Eu^{3+} favours quenching of the luminescence. The longer lifetime in $CHCl_3$ and

DCM are because of the frequency of C–H vibrational oscillators is lower than that of O–H.

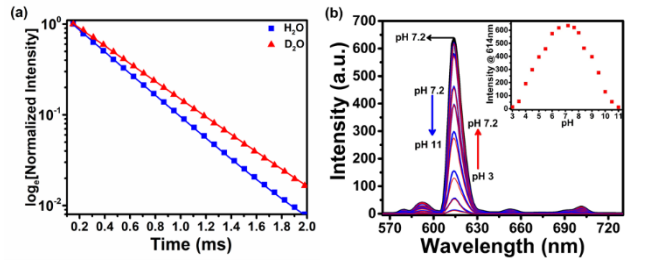

Figure 4. Luminescence decay profile of $^5D_0$ excited state at 614 nm in H_2O and D_2O under ambient condition for [Eu(tta)$_3$(naptpy)] (**1**) from at T = 298 K, λ_{ex} = 349 nm, [**1**] = 3 μM, delay and gate time = 0.1 ms, total decay time = 10 ms, Ex. and Em. slit width = 5 nm. Red and blue curves are single exponential fitting curve in H_2O and D_2O respectively. (b) The changes in Eu^{3+} emission of [Eu(tta)$_3$(naptpy)] (**1**) in 5 mM Tris-buffer as a function of pH, showing switched *'off-on-off'* upon basification, λ_{ex} = 349 nm. Inset: the change in $^5D_0 \rightarrow {}^7F_2$ emission intensity of [Eu(tta)$_3$(naptpy)] (**1**) monitored at 614 nm as a function of pH (blue traces = basic pH, red traces = acidic pH).

To gain an appreciation of the solution state speciation of complex **1** in aqueous media, excited state lifetimes in H_2O and D_2O were recorded that allows determination of hydration number (q) of the complex *via* modified Horrock's equation ignoring any alternative deactivation pathway (Fig. 4a).[34] The determined q < 1 for the complex **1** confirms absence of any bound H_2O to Eu^{3+} in solution. This coordinnative saturation restricts the energy dissipation by VET from Eu^{3+} to the O−H oscillator and enhances the emissive lifetime of the probe.

Table 2. Selected photophysical data of [Eu(tta)3(naptpy)] (**1**)

λ_{max} [nm],[a] (ε [M^{-1}cm^{-1}])	τ [ms] [b]						q[c]
	$CHCl_3$	THF	DMF	DCM	H_2O	D_2O	
285 (56,820), 349 (64,200)	0.652	0.528	0.498	0.599	0.365	0.440	0.26

[a] UV-vis spectrum in aq. DMF. [b] Luminescence lifetimes ($\tau \pm 15\%$). [c] Hydration number ($q \pm 10\%$) determined using modified Horrock's equation.[34]

pH response on Photoluminescence

Luminescence properties of Eu(III)-β-diketonate complex **1** was expected to be very sensitive to pH changes due to the presence of α-acidic proton in tta ligand. Generally acidic sites are responsible for quenching of luminescence intensity of lanthanide complexes.[37,38] This leads us to expect that complex **1** having three β-diketonate moieties could also be used as pH measuring probe. To further evaluate the potential sensing applications of complex **1** as pH probe, the changes in emission intensity at various pH ranges were examined. The emission intensity of **1** (λ_{ex} = 349 nm) was quenched with changes in pH due to the protonation of the α-proton of tta.

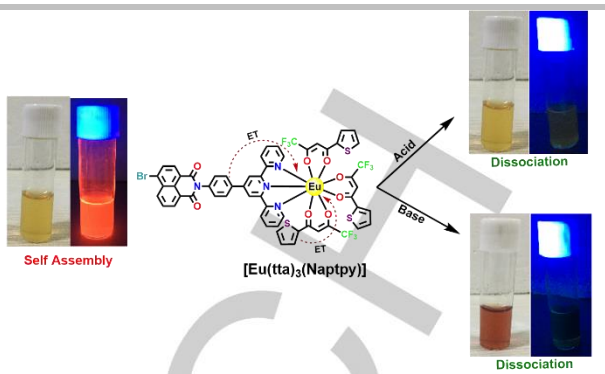

Figure 5. Proposed schematic representation and visible color changes of the luminescent complex **1** at pH 7.2 showing red Eu^{3+} emission (self-assembly) and the dissociation of complex **1** in acidic and alkaline solution at pH 2 and pH 11 respectively. Photographs of complex **1** in different conditions under ambient (left) and UV light exposure (right) respectively.

The pH-sensing mechanism of [Eu(tta)$_3$(naptpy)] (**1**) demonstrate that characteristic luminescence intensity of Eu^{3+} ($^5D_0 \rightarrow {}^7F_2$) would be reduced immediately as H^+ can break the six-membered chelate ring built by tta and Eu^{3+}, which deteriorate the sensitization mechanism of β-diketonate and consequently results in poor energy transfer to Eu^{3+} (Fig. 4b). Thus at lower acidic pH the ternary complex **1** dissociate to form a solvent bound complex with mostly significant quenching by VET (Fig. 5, S7). In addition, the response rate to the pH changes must be considered for the luminescence-based pH detecting systems. As both protonation and deprotonation are instantaneous reversible chemical processes, the luminescence change occurs immediately, thus considered as a real-time measurement. The reversibility of a pH probe is a very important and necessary criterion. To test this reversible response for probe **1**, the pH of the solution was switched back and forth between 7.5 and 2.5 by using HCl and Et_3N (Fig. S8, SI). Results clearly show that the probe exhibited a highly reversible response to pH and the response time is instantaneous. The switching between the luminescence ON/OFF states could thus be repeated for multiple cycles. The luminescence response of **1** can be recovered completely after exposure to the Et_3N due to the formation of complex **1** by self-assembly in solution.

In neutral pH 7.2, complex **1** shows strong red emission while in either acidic (pH < 4) or alkaline solution (pH > 9) luminescence is quenched as the tta moiety get dissociated from ternary complex **1**. It might be possible that on dissociation of complex some solvent molecules or anions were displacing β-diketone moiety which results in quenching of Eu^{3+}-emission via nonradiative vibrational energy transfer (VET). Moreover, a decrease in Eu^{3+} emission intensity was also evident under UV lamp as directly seen in Fig. 5. The changes in absorption spectra of [Eu(tta)$_3$(naptpy)] (**1**) as a function of pH also displayed significant changes suggesting a possible dissociation of tta ligands and scope of further ligand-exchange reactions (Fig. S9, SI).

Displacement based anion sensing

Reversible displacement of tta in complex **1** in the presence of competitive coordinating ligands, especially anions could be applied as a potential sensing strategy.[38-40] This can be termed as lanthanide based 'displacement assays' where Eu^{3+} emission was anticipated to be quenched as energy transfer from antenna would be prevented upon displacement of β-diketonate moiety.[41] Thus, the binding of anions to the inner-sphere of Eu^{3+} brings significant changes in the intensity of the hypersensitive $^5D_0$ emissive peak of Eu^{3+}. This hallmark makes the complex **1** ideal for the development of luminescent sensor for coordinating

anions. Quantitative titrations in the presence of various anions with [Eu(tta)$_3$(naptpy)] at pH 7.2 were performed to assess this assumption. The result illustrates that luminescence intensity of Eu^{3+} at 614 nm does not affect much upon addition of anions such as Br^-, ClO_4^- and PF_6^- to [Eu(tta)$_3$(naptpy)] (**1**) while NO_2^- and I^- offers only small changes in Eu^{3+} emission intensity at 614 nm (Fig. S10 and S11, SI). In contrast, the presence of citrate, F^-, acetate, tartaric acid, HCO_3^-, and ascorbate results in significant decrease in luminescent intensity of Eu^{3+} at 614 nm as shown in Fig. 6 and Fig. 7.

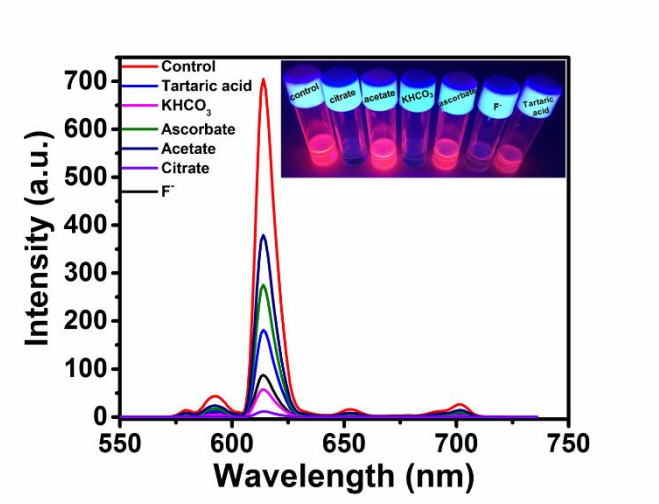

Figure 6. Luminescence spectral changes of complex **1** with tartarate, HCO_3^-, ascorbate, CH_3COO^-, citrate and F^- (as their sodium or TBA salt). λ_{ex} = 349 nm; [**1**] = 10 μM; [Anions] = 20 μM; Ex. and Em. slit width = 5.0 nm, T = 298 K. Inset shows digital photographs of complex **1** under UV lamp (λ= 365 nm) showing intensity changes for corresponding anions.

Furthermore, these changes are clearly visible by the naked eye under UV lamp (Fig. 6). Detailed quantitaive anion titration using sodium citrate, tartaric acid and $NaHCO_3$ were also performed at pH 7.2 which clearly confirms that Eu^{3+} emission decresed gradually *via* displacement of tta (Fig. S12, SI). These observations indicates oxophillicity and stronger binding affinity of oxoanions with hard Eu^{3+} centre. The present probe although lack very high specificity to a particular anion, which could be achieved *via* appropriate modification of the ligand framework. This system and current strategy although proves itself as potential platform for luminescent Ln-based displacement assay for various anions.

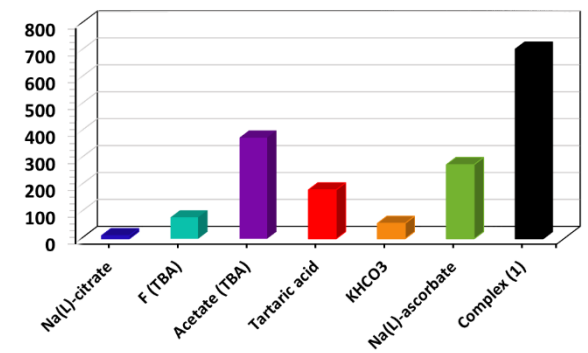

Figure 7. The emission intensity contrast bars of [Eu(tta)$_3$(naptpy)] (**1**) (10 μM, λ_{ex} = 349 nm) upon addition of anions (tartrate, HCO_3^-, ascorbate, CH_3COO^-, citrate and F^-) at λ_{em} = 614 nm at pH 7.2. The tertiary complex **1** is shown for comparison.

DNA binding studies

DNA is the vital pharmacological target for various metal-based chemotherapeutic drugs like cisplatin, carboplatin or oxaliplatin where they mainly bind with the nitrogen of nucleobases of DNA and trigger cell-death pathways. The non-covalent DNA binding agents are either intercalators or groove binders. The presence of planar naptpy moiety encouraged us to study the DNA-binding propensity of the complex **1** using various spectroscopic techniques.[42,43]

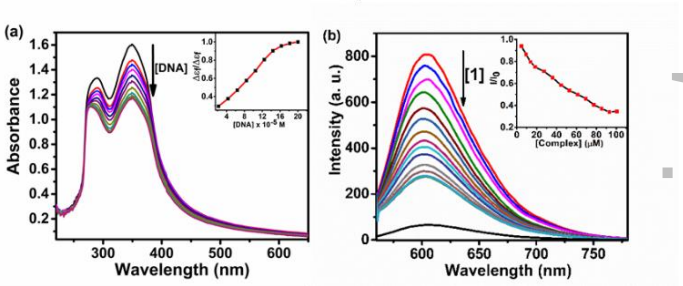

Figure 8. (a) Absorption spectral traces of [Eu(tta)$_3$(naptpy)] (**1**) (15 μM) in 5 mM Tris-buffer (pH 7.2) with increasing [CT- DNA] at 298 K. Inset: $\Delta\varepsilon_{af}/\Delta\varepsilon_{bf}$ vs. [DNA] plot for complex **1**. (b) Emission spectral traces of EB-bound CT-DNA with increasing [**1**] in 5 mM Tris-buffer (pH 7.2) at 298 K. λ_{ex}= 546 nm, λ_{em} = 603 nm, [EB] = 13.5 μM. Inset: plot of I/I_0 *vs.* [complex].

Absorption spectroscopy. The binding propensity of complex **1** with CT-DNA was studied by UV-vis spectral titrations. The intercalation results in a bathochromic shift and hypochromism due to possible perturbation of the π-orbitals of DNA base pairs with the π-orbitals of the intercalated ligand.[42] The absorption spectral traces of complex **1** with increasing concentration of CT-DNA is shown in Fig. 8a. The intrinsic DNA binding constant (K_b) of the complex **1** was obtained by monitoring the changes in absorbance of the complex with increasing DNA concentrations.[43] The calculated K_b value for complex **1** in the range of 10^4 M^{-1} suggests groove binding or partial intercalation through naptpy and tta moiety with the DNA (Table 3).

Emission quenching method. Ethidium bromide (EB) is a well-known intercalating dye used as a fluorescent tag which shows intense emission upon binding to duplex-DNA. The displacement of EB by competitive titration with **1** leads to decrease in the emission intensity of EB at 603 nm suggesting intercalative or minor groove binding modes for **1** (Fig. 8b). The extent of decrease in fluorescence intensity gives a measure of the relative binding affinity of the complex. The calculated K_{app} of 10^6 M^{-1} for the probe indicates it's strong binding affinity with DNA.

Serum protein binding studies

Serum albumins are the major (~55%) and most extensively studied transport proteins present in circulatory system. BSA is a model protein for physicochemical and biophysical studies as it serves as a transporter of many organic molecules, steroids, fatty acids, thyroid hormones, and many drugs to their target. The binding interaction of Eu^{3+} complex with BSA was monitored using quenching of tryptophan (Trp-134 and Trp-212) emission intensity.[44] With gradual increase in concentration of complex **1** the fluorescence intensity at 345 nm gets quenched steadily indicating a binding interaction between complex **1** and BSA (Fig. 9).

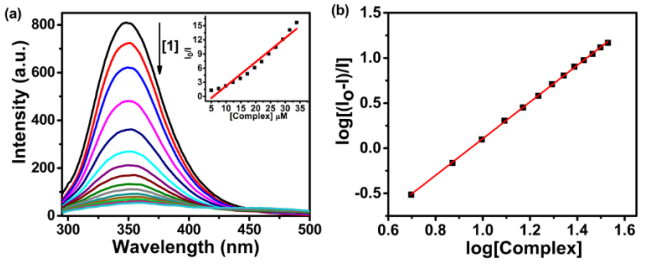

Figure 9. (a) The effect of addition of [Eu(tta)$_3$(naptpy)] (**1**) on fluorescence quenching of BSA in 5 mM Tris-buffer (pH 7.2) at 298 K. The inset shows the plot of I_0/I vs. [complex] for complex **1**. λ_{ex} = 295 nm, λ_{em}= 345 nm, [BSA] = 2 μM. (b). Scatchard plots of log[$(I_0 - I)/I$] vs. log[complex] to determine the binding constant (K), quenching rate constant (k_q) and number of binding site (n) for BSA to complex interaction.

The remarkable quenching may be attributed to the various changes in the BSA secondary structure, such as ground state complex formation, a collision between fluorophores and quenchers, protein denaturation, or conformational changes of the protein induced by these quenchers.[45] The Stern-Volmer equation and Scatchard plots were used to dtermine the Stern-Volmer quenching constant for BSA fluorescence (K_{BSA}) for [Eu(tta)$_3$(naptpy)] (**1**).[44] The plots were shown in Fig. 9 and values are listed in Table 3. The K_{BSA} value (10^5 M^{-1}) indicate the strong affinity of complex **1** to serum proteins.

Table 3. Binding interaction parameters for the [Eu(tta)$_3$(naptpy)] (**1**) complex with CT-DNA and BSA

[Eu(tta)$_3$(naptpy)] (**1**)	K_b/M^{-1}[a]	K_{app}/M^{-1}[b]	K_{BSA}/M^{-1}[c]	k_q/M^{-1}[d]	K/M^{-1}[e]
	6.53 X 10^4	2.21 x 10^6	5.09 X 10^5	5.09 X 10^{13}	1.93 X 10^6

[a] K_b intrinsic DNA binding constant with calf-thymus DNA. [b] K_{app} apparent DNA binding constant. [c] K_{BSA} Stern-Volmer quenching constant for BSA fluorescence. [d] kq quenching rate constant. [e] K binding constant with BSA. Number of binding sites (n) are 2.03.

DNA sensing studies

Due to unrivalled optical properties originating from the f→f transitions in the inner 4f shell of Ln^{3+}, lanthanide complexes are ideal luminescent probes for an array of numerous applications in sensing and detection of various analytes and biological targets.[16,36]

To investigate the sensing ability of complex **1** towards DNA, the time-delayed luminescence spectra was recorded in presence of CT-DNA. The significant quenching of the Eu-centered luminescence ($^5D_0 \rightarrow {}^7F_J$ transitions) was obeserved on addition of CT-DNA to the complex **1** (Fig. 10). The notable quenching of hypersensitive peak (ΔJ =2) of Eu^{3+} at 614 nm indicates the possible alteration of direct bonding in the primary coordination sphere of Eu^{3+}. The luminescence quenching of complex **1** by DNA indicated that complex had a strong interaction with DNA possibly through the binding of negatively charged oxygen atoms of phosphate (PO_4^{3-}) and displacement of tta as antenna which leads to poor sensitization of the probe by static or nonradiative vibrational quenching.[30]

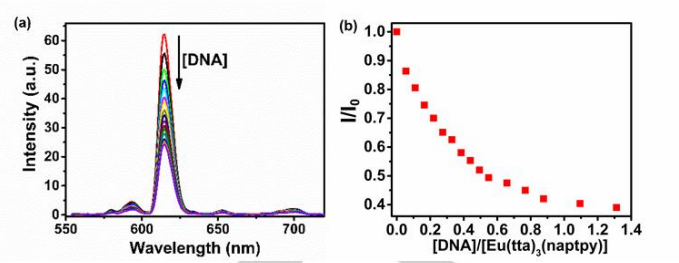

Figure 10. (a) Time-delayed luminescence spectra of [Eu(tta)$_3$(naptpy)] (**1**) showing luminescence intensity quenching with increasing concentration of CT-DNA in 5 mM Tris buffer (pH=7.2) at 298 K [delay time = gate time = 0.1 ms, λ_{ex} = 349 nm, Ex. and Em. slit width = 5 nm]. (b) Luminescence emission intensity of complex **1** at 614 nm vs. the [CT-DNA]/[**1**] ratio.

Conclusions

In summary, a highly stable luminescent complex [Eu(tta)$_3$(naptpy)] (**1**) with a sensitized light absorbing chromophores *viz.* tta and naptpy, have been prepared and their solution state behavior have been thoroughly characterized using a combination of ^{1}H-NMR, IR, ESI-MS, UV/Vis and emission spectroscopy. Complex **1** shows characteristic strong red luminescence both in solution and solid state, which suggests efficient excited state energy transfer from the antenna moieties to the Eu^{3+} or $^5D_0$ state with long excited state lifetime in milliseconds. We have shown that the ternary complex **1** is highly pH sensitive and further it can be used as a luminescent sensor for anions at physiological pH, where tta (β-diketone) moiety is displaced by oxyanions with gradual decreases in the Eu^{3+} emission. Furthermore, complex **1** shows effective binding tendency with CT-DNA *via* groove binding or partial intercalation through naptpy and tta moiety. It also strongly binds with BSA as determined through emission quenching studies and may be suitable to transport the Eu^{3+} probe to the pathological site for its delivery. The remarkable photostability, the absence of inner-sphere water ($q < 1$), and longer excited-state lifetimes (ms) and high luminescence under biological pH window of the complex make them an ideal platform for intracellular pH measurement probes.

Experimental Section

Materials and methods

All the chemicals and reagents were purchased from Sigma-Aldrich, Alfa Aesar and used without further purification unless otherwise stated. The naptpy ligand was prepared using 4-bromo-1,8-naphthalic anhydride and 4'-(4-aminophenyl)-2,2':6',2''-terpyridine (Tpy-NH_2). Solvents used were either HPLC grade or were purified by standard procedures.

The FTIR spectra were collected with a Perkin-Elmer Model 1320 FT-IR spectrometer. Electronic spectra were measured at 298 K using a Perkin-Elmer Lambda 25 UV-Vis spectrophotometer. ^{1}H-NMR spectra were recorded at 298 K on a JEOL-ECX 500 FT (400 MHz) instrument with chemical shift-referenced to tetramethylsilane (TMS). ESI-MS measurements were carried out

using a WATERS Q-TOF Premier mass spectrometer. The steady-state fluorescence and time-delayed luminescence spectra were recorded using Agilent Cary eclipse fluorescence spectrophotometer at 298 K.

Lifetime measurements were achieved under ambient conditions in pure DMF, H_2O, D_2O (contains 1% DMF), $CHCl_3$, DCM and THF using a pulsed Xenon lamp at λ_{ex} = 349 nm and λ_{em} = 614 nm for Eu^{3+} complex **1** with a delay and gate time of 0.1 ms. Decay curves were fitted by non-linear least square method. Lifetime data for [Eu(tta)$_3$(naptpy)] (**1**) under various conditions were shown in Fig. 4a and Fig. S6, SI. The excited state lifetime measurements in water and D_2O allowed the determination of the number of water molecules (q) directly coordinated to the Eu^{3+} using the following modified Horrocks' equations for Eu^{3+}.[34]

$$q_{Eu} = 1.2\left(\frac{1}{\tau_{H_2O}} - \frac{1}{\tau_{D_2O}} - 0.25\right)$$

All the theoretical calculations were done using Gaussian 09 and applying density functional theory (DFT). Ligand structure was optimized using B3LYP/6-31G level of theory in the gas phase.[32] Ground states of both the singlet (S_0) and first triplet state (T_1) were optimized using their respective spin multiplicities. Excited states of both singlet and triplet state were calculated using time-dependent density functional theory (TD-DFT) method with the pre-optimized ligand structure using B3LYP/6-31G level of theory [32], and simulated absorbance spectra are generated (Fig. S13 and Fig. S14, SI).

Synthesis and characterization

4'-(4-Nitrophenyl)-2,2',6,2''-terpyridine (Tpy-NO_2) and Eu(tta)$_3$(H_2O)$_2$] were prepared according to the reported procedure in the literature (Scheme 2).[46,47]

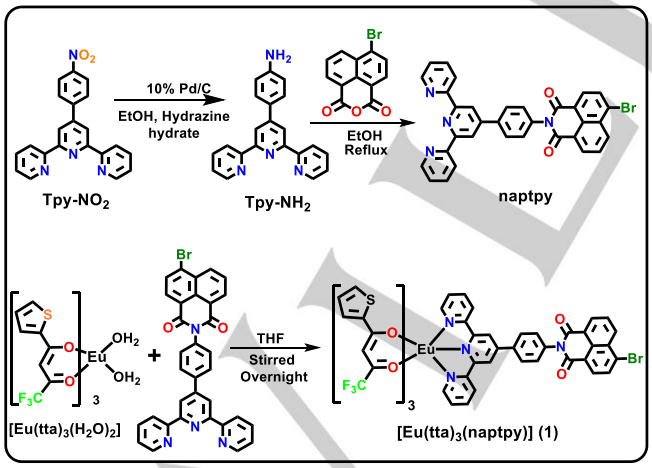

Scheme 2. General synthetic scheme for naptpy ligand and [Eu(tta)$_3$(naptpy] (**1**).

4'-(4-aminophenyl)-2,2',6,2''-terpyridine (Tpy-NH_2).

A solution of 4'-(4-nitrophenyl)-2,2',6,2''-terpyridine (708 mg, 2.0 mmol) in the presence of 10% Pd/Charcoal catalyst (300 mg) in absolute ethanol (100 mL) was refluxed for 1.5 h. Hydrazine monohydrate (3.2 mL, 56.4 mmol) in absolute ethanol (40 mL) was then added dropwise to the reaction mixture and refluxed for 5 h. The resulting solution was then filtered over celite or cotton wool, and the catalyst was washed with dichloromethane (200 mL). The organic phase was washed with water (4 X 100 mL). The organic phase was then dried over Na_2SO_4 and solvent was removed in vacuo to yield 4'-(4-aminophenyl)-2,2',6,2''-terpyridine as yellow crystals. (Yield: 514 mg, 79%), ^{1}H-NMR (400 MHz, $CDCl_3$) d (ppm): 8.73 (2H, d), 8.69 (2H, s), 8.66 (2H, d), 7.87 (2H, m), 7.79 (2H, d), 7.34 (2H, m), 6.80 (2H, d), ESI-MS (*m/z*) (%): $[M+H]^+$ calcd for $C_{21}H_{17}N_4$: 325.1453, Found, 325.1459.

2-(4-([2,2':6',2''-terpyridin]-4'-yl)phenyl)-6-bromo-1H benzo[de]isoquinoline-1,3(2H)-dione (naptpy).

4-Bromo-1,8-napthalic anhydride (277 mg, 1.0 mmol) and $TpyNH_2$ (324 mg, 1.0 mmol) in 30 mL ethanol were heated to reflux for 24 h. Solvent was removed in vaccuo then washed with water. A yellow coloured product was obtained, which was further recrystallized from hot glacial acetic acid to afford the target compound as a yellow powder. The yellow solid was then filtered and washed with cold water and finally dried in vacuum over P_4O_{10}. (Yield: 532 mg, 91 %). UV/Vis (DMF, 298 K): λ_{max}, nm, (ε, $LM^{-1}cm^{-1}$): 282 (62,150), 329 (53,500), ^{1}H-NMR (400 MHz, $CDCl_3$) d (ppm): 8.79 (2H, d), 8.77 (2H, s), 8.75 (1H, d), 8.68 (3H, m), 8.66 (1H, d), 8.48 (1H, d), 8.42 (t, 1H), 8.11 (2H, dd), 8.09 (m, 2H), 7.91 (2H, dd), 7.88 (2H, m), ESI-MS in DMF (*m/z*) (%): $[M+H]^+$, Calcd for $C_{33}H_{20}Br_1N_4O_2$: 583.077, Found: 583.077.

Synthesis of [Eu(tta)$_3$(naptpy)] (1)

To a stirred solution of naptpy (70 mg, 0.12 mmol) in 15 mL THF, [Eu(tta)$_3$(H_2O)$_2$] (85.19 mg, 0.1 mmol) was added. The reaction mixture was stirred overnight at RT. The resulting solution was evaporated in vaccuo. The residue was re-dissolved in minimum amount of THF and addition of n-hexane led to the precipitation of brown-yellow microcrystalline powder as the target compound [Eu(tta)$_3$(naptpy)] (**1**). (Yield: 100 mg, 72 %), UV/Vis (aqueous-DMF, 298 K): λ_{max}, nm, (ε, $LM^{-1}cm^{-1}$): 285 (56,820), 349 (64,200), ESI-MS in DMF; (*m/z*) (%): ([M-tta]$^+$ Calcd for $C_{49}H_{27}Br_1F_6N_4O_6S_2Eu_1$: 1176.97 (100), 1174.97 (43), 1175.97 (24), 1177.97 (54), 1178.97 (70), 1179.97 (34). Found: 1176.9730 (100), 1174.9711 (46), 1175.9727 (25), 1177.9750 (53), 1178.9740 (75), 1179.9760 (37).

DNA binding experiment

DNA binding experiment was done in Tris–HCl/NaCl buffer (5 mM Tris–HCl/NaCl, pH 7.2) using complex **1** in DMF solution. CT-DNA in the buffer medium gave the ratio of 1.9:1 of absorbance in UV region at wavelength 260 and 280 nm which showed that DNA is free from protein. The DNA concentration was obtained using ε_{260} = 6600 $M^{-1}cm^{-1}$.[48] Absorption spectral titrations were performed by varying the concentration of CT-DNA while keeping the complex concentration constant. Due to the corrections made for the absorbance of CT-DNA itself (Fig. 8a). The equilibrium binding constant (K_b) of the complex **1** was determined by the following equation.[43]

$$[DNA]/(\varepsilon_a - \varepsilon_f) = [DNA]/(\varepsilon_b - \varepsilon_f) + 1/K_b(\varepsilon_b - \varepsilon_f)$$

Where [DNA] is the concentration of CT-DNA in base pairs, ε_a is the apparent extinction coefficient, ε_f and ε_b refers to the extinction

coefficients of the complex in its free and fully bound form. The K_b values are obtained from the [DNA]/(ε_a-ε_f) vs. [DNA] plots.

Protein binding experiments

The interaction of the complex **1** with bovine serum albumin (BSA) has been studied from tryptophan emission quenching experiments. The quenching of the emission signals at 340 nm (λ_{ex}= 295 nm) were recorded by increasing concentration of complex **1** in DMF solution to the solution of BSA (2 μM) in 5 mM Tris-HCl-NaCl buffer (pH 7.2) Fig. 9a. The quenching constant (K_{BSA}) has been determined quantitatively by using Stern–Volmer equation (Fig. 9).[44]

Stern–Volmer I_0/I vs. [complex] plots were made using the corrected fluorescence data taking into account the effect of dilution. Linear fit of the data using the equation:

$$I_0/I = 1 + K_{BSA}[Q]$$

where, I_0 and I are the emission intensities of BSA in the absence of quencher and in the presence of quencher of concentration [Q], gave the quenching constants (K_{BSA}).

pH Titration

The luminescence titration of complex **1** (1 mM) have been examined at different pH in 5 mM Tris–HCl/NaCl buffer by performing acid–alkali (1M HCl and 1M NaOH) titration experiment through both absorption and emission luminescence spectroscopy. To observe the changes in luminescence emission intensity, $^5D_0 \rightarrow {}^7F_2$ transition of Eu^{3+} complex **1** was monitored with gradual changes in pH.

Anion Sensing

Luminescence spectroscopy is valuable tool to illustrate the nature of anion binding to the Eu^{3+}. The titrations with various anions with complex **1** were done by adding aqueous solution of anions in 2 mL aliquots to a solution of complex **1** in DMF:H_2O (70%). To avoid pH changes upon addition to the anions, the anion stock solutions were adjusted to pH 7.2 prior to addition to the complex **1**.

Acknowledgements

We thank Science and Engineering Research Board (SERB) (EMR/2016/000521), Government of India for financial support. KG thanks the University Grant Commission (UGC) for research fellowship. We thank Amitosh Sharma for helping in DFT calculations.

Keywords: Lanthanide• luminescence • europium • pH sensing • anion sensing

[1] a) P. A. Gale, R. Quesada, *Coord. Chem. Rev*. **2006**, *250*, 3219–3244; b) S. Shinoda, H. Tsukube, *Analyst*, **2011**, *136*, 431–435; c) D. Parker, *Chem. Soc. Rev*. 2004, **33**, 156-165.

[2] U. Reddy, G., R. Lo, S. Roy, T. Banerjee, B. Ganguly, A. Das, *Chem. Commun*. **2013**, *49*, 9818–9820.

[3] a) Y. Bretonniere, M. J. Cann, D. Parker, R. Slater, *Org. Biomol. Chem.* **2004**, *2*, 1624-1632; b) A. Thibon, V. C. Pierre, *J. Am. Chem. Soc.* **2009**, *131*, 434-435; c) R. Pal, D. Parker, L. C. Costello, *Org. Biomol. Chem.* **2009**, *7*, 1525-1528; d) S. J. Butler, B. K. McMahon, R. Pal, D. Parker, J. W. Walton, *Chem. Eur. J.* **2013**, *19*, 9511-9517.

[4] a) S. J. Butler, D. Parker, *Chem. Soc. Rev.* **2013**, *42*, 1652– 1666; b) L. J. Charbonniere, R. Ziessel, M. Montalti, L. Prodi, N. Zaccheroni, C. Boehme, G. Wipff, *J. Am. Chem. Soc*. **2002**, *124*, 7779.

[5] a) H. Tsukube, S. Shinoda, *Chem. Rev.* **2002**, 102, 2389; b) T. Yamada, S. Shinoda, H. Tsukube, *Chem. Commun.* **2002**, 1218-1219; c) H. Tsukube, T. Yamada, S. J. Shinoda, *Alloys Compd.* **2004**, 374, 40; d) M. D. Best, E. V. Anslyn, *Chem. sEur. J*. **2003**, 9, 51; e) M. Montalti, L. Prodi, N. Zaccheroni, L. J. Charbonnie`re, L. Douce, R. Ziessel, *J. Am. Chem. Soc*. **2001**, *123*, 12694.

[6] a) D. Parker, *Coord. Chem. Rev.* **2000**, *205*, 109–130; b) J. I. Bruce, R. S. Dickins, L. J. Govenlock, T. Gunnlaugsson, S. Lopinski, M. P. Lowe, D. Parker, R. D. Peacock, J. J. B. Perry, S. Aime, M. Bott., *J. Am. Chem. Soc.* **2000**, *122*, 9674–9684; c) J. Yu, D. Parker, *Eur. J. Org. Chem.* **2005**, 4249–4252.

[7] a) J. P. Leonard, C. M. G. dos Santos, S. E. Plush, T. McCabe, T. Gunnlaugsson, *Chem. Commun.* **2007**, 129-131; b) A. B. Aletti, D. M. Gillen, T. Gunnlaugsson, *Coord. Chem. Rev.* **2018**, *354*, 98-120.

[8] a) J.-C. G. Bünzli, S. V. Eliseeva, *Basics of Lanthanide Photophysics. In Lanthanide Luminescence: Photophysical, Analytical, and Biological Aspects*; b) P. Hänninen, H. H. Härmä, Eds.; *Springer Series on Fluorescence, Springer-Verlag: Berlin*, **2011**, *7*, 1−45.

[9] a) G. A. Crosby, R. E. Whan, R. M. Alire, *J. Chem. Phys*. **1961**, *3*, 743−748; b) S. Comby, J.-C. G. Bünzli, *In Handbook on the Physics and Chemistry of Rare Earths*, vol. 37; c) K. A. Gschneidner, J.-C. G. Bünzli, V. K. Pecharsky, Elsevier, North Holland, **2007**.

[10] a) J.-C. G. Bünzli, C. Piguet, *Chem. Soc. Rev*. **2005**, *34*, 1048-1077; b) e) H. Tsukube, S. Shinoda, H. Tamiaki, *Coord. Chem. Rev*. **2002**, *226*, 227.

[11] a) R. Pal, D. Parker, *Chem. Commun.* **2007**, 474-476; b) R. Pal, D. Parker, *Org. Biomol. Chem.* **2008**, *6*, 1020-1033; b) B. S. Murray, E. J. New, R. Pal, D. Parker, *Org. Biomol. Chem.* **2008**, *6*, 2085-2094.

[12] a) C. P. McCoy, *Chem. Mater*. **2006**, *18*, 4336-4343; b) H. Tsukube, S. Shinoda, *Chem. Rev*. **2002**, *102*, 2389.

[13] a) D. G. Smith, B. K. Mcmahon, R. Pal, D. Parker, *Chem. Commun.* **2012**, *48*, 8520-8522; b) E. J. New, D. Parker, D. G. Smith, J. W. Walton, *Curr. Opin. Chem. Biol.* **2010**, *14*, 238-246.

[14] a) S. Gupta, S. Mondal, A. Mhamane, A. Datta, *Inorg. Chem.* **2013,** *52*, 12314-12316; b) A. Datta, J. M. Hooker, M. Botta, M. B. Francis, S. Aime, K. N. Raymond, *J. Am. Chem. Soc.* **2008**, *130*, 2546-2552.

[15] a) S. I. Klink, G. A. Hebbink, L. Grave, P. G. B. Oude, F. C. J. M. van Veggel, M. H. V. Werts, *J. Phys. Chem. A,* **2002,** *106*, 3681; b) P. Sutar, V. M. Suresha, T. K. Maji, *Chem. Commun.* **2015**, *51*, 9876-9879; c) S. Roy, A. Chakraborty, T. K. Maji, *Coord. Chem. Rev*. **2014**, *273*, 139-164.

[16] a) A. Chandra, K. Singh, S. Singh, S. Sivakumar, A. K. Patra, *Dalton Trans*. **2016**, *44*, 19844-19855; b) K. Singh, S. Banerjee and A. K. Patra, *RSC Adv.* **2015**, *5*, 107503-107513; c) K. Singh, S. Singh, P. Srivastava, S. Sivakumar, A. K. Patra, *Chem. Commun.* **2017**, *53*, 6144-6147.

[17] a) S. Dasari, A. K. Patra, *Dalton Trans*. **2015**, *44*, 19844-19855; b) S. Dasari, S. Singh, S. Sivakumar, A. K. Patra *Chem. Eur. J.* **2016**, *22*, 17387-7396; (c) Z. Abbas, S. Dasari, A. K. Patra, *RSC Adv.* **2017**, *7*, 44272-44281

[18] a) N. S. Baek**,** M. K. Nah, Y. H. Kim, H. K. Kim, *J. Lumin.* **2007,** *127*, 707–712; b) R. K. Mahajan, I. Kaur, R. Kaur, S. Uchida, A. Onimaru, S. Shinoda, H. Tsukube, *Chem. Commun*. **2003**, 2238-2239; c) J. Lehr, P. D. Beer, S. Faulkner, J. J. Davis., *Chem. Commun*. **2014**, *50***,** 5678—5687; d) C. S. Bonnet, J. Massue, S. J. Quinn, T. Gunnlaugsson, *Org. Biomol. Chem*. **2009**, *7*, 3074.

[19] a) C. Yang, J. Xu, J. Ma, D. Zhu, Y. Zhang, L. Lianga, M. Lu, *Polym. Chem.,* **2012***, 3*, 2640; b) Z. Li, P. Li, Q. Xu, H. Li., *Chem. Commun.,* **2015***, 51*, 10644-10647. c) H.-Y. Wong, W.-S. Lo, W. T. K. Chan, G.-L. Law *Inorg. Chem.* **2017**, *56*, 5135−5140; d) J. Li, L. Wang, X. Liu, X. Jiang, Y. Cheng, C. Zhu, *Polym. Chem.*, **2012**, *3*, 2578–2582.

[20] a) D. Ghosha, M. N. Luwang, *RSC Adv.,* **2015**, *5*, 47131–47139; b) X. Li, D. Zhang, J. Li., *Spectrochimica Acta Part A: Molecular and Biomolecular Spectroscopy*, **2014**, *127***,** 1–9. c) C. Yang, J. Xu, J. Ma, D. Zhu, Y. Zhang, L. Lianga, M. Lu, *Photochem. Photobiol. Sci*., **2013**, *12*, 330–338. d) D.

V. Kazakov, F. E. Safarov, *Photochem. Photobiol. Sci*., **2014**, *13*, 1646–1649.

[21] a) O. Kotova, R. Daly, C. M. G. dos Santos, M. Boese, P. E. Kruger, J. J. Boland and T. Gunnlaugsson, *Angew. Chem., Int. Ed*., **2012**, *51*, 7208–7212; b) A. Wild, A. Winter, F. Schlutter, U. S. Schubert, *Chem. Soc. Rev*. **2011**, *40*, 1459; c) U. S. Schubert, H. Hofmieier, G. R. Newkome, *Modern Terpyridine Chemistry*, Wiley-VCH, Weinheim, **2006**.

[22] a) W. S. Lo, W. M. Kwok, G. L. Law, C. T. Yeung, C. T. L. Chan, H. L. Yeung, H. K. Kong, C. H. Chen, M. B. Murphy, K. L. Wong and W. T. Wong, *Inorg. Chem*., **2011**, 50, 5309– 5311; b) R. Shunmugam and G. N. Tew, *J. Am. Chem. Soc*., **2005**, 127, 13567–13572; c) B. Song, G. L. Wang, M. Q. Tan and J. L. Yuan, *J. Am. Chem. Soc*., **2006**, 128, 13442–13450.

[23] a) J. Costa, R. Ruloff, L. Burai, L. Helm and A. E. Merbach, *J. Am. Chem. Soc.*, **2005**, 127, 5147–5157; b) N. Chandrasekhar and R. Chandrasekar, *J. Org. Chem.*, **2010**, *75*, 4852–4855; c) C. L. Yang, J. Xu, Y. F. Zhang, Y. W. Li, J. Zheng, L. Y. Liang and M. G. Lu, *J. Mater. Chem. C*, **2013**, *1*, 4885–4901.

[24] a) I. Grabchev, P. Meallier, T. Konstantmova, M. Popova, *Dyes Pigm*. **1995**, *28*, 41– 46; b) Z. Cao, P. Nandhikonda, M.D. Heagy, *J. Org. Chem.* **2009**, *74*, 3544–3546; c) C. S. Bonnet, M. Devocelle and T. Gunnlaugsson, *Chem. Commun*., **2008**, 4552; d) D. R. Kauffman, C. M. Shade, H. Uh, S. Petoud and A. Star, *Nat. Chem*., **2009**, *1*, 500; e) M. de Sousa, M. Kluciar, S. Abad, M. A. Miranda, B. de Castro and U. Pischel, *Photochem. Photobiol. Sci*., **2004**, *3*, 639-642; f) G. J. Ryan, S. Quinn, T. Gunnlaugsson, *Inorg. Chem*. **2008**, *47*, 401-403.

[25] a) D. Srikun, E.W. Miller, D.W. Domaille, C.J. Chang, *J. Am. Chem. Soc*. **2008**, *130*, 4596-4597; b) E.B. Veale, T. Gunnlaugsson, *J. Org. Chem*. **2008**, *73*, 8073-8076.; c) R. Shunmugam, G. N. Tew, *Chem. Eur. J.* **2008**, *14*, 5409-5412; d) L. Lin-Bo, J. Shun-Jun, L. Wei-Hong, *Chin. J. Chem.*, **2008**, *26*, 417-420; e) C. S. Bonnet, M. Devocelle, T. Gunnlaugsson, *Org. Biomol. Chem.,* **2012**, *10*, 126–133; f) J. Zhou, C. Fang, Y. Liu, Y. Zhao, N. Zhang, X. Liu, F. Wang, D. Shangguan, *Org. Biomol. Chem*. **2015**, *13*, 3931–3935.

[26] a) A. J. Amoroso, S. J. A. Pope, *Chem. Soc. Rev*. **2015**, *44*, 4723-4742; b) S. J. Butler, L. Lamarque, R. Pal, D. Parker, *Chem. Sci.* **2014**, *5*, 1750-1756.

[27] a) A. Thibon, V. C. Pierre, *Anal. Bioanal. Chem.* **2009**, *394*, 107-120; b) M. Delbianco, V. Sadovnikova, E. Bourrier, G. Mathis, L. Lamarque, J. M. Zwier, D. Parker, *Angew. Chem. Int. Ed*. **2014**, *53*, 10718-10722; *Angew. Chem.* **2014**, *126*, 10894-10898.

[28] (a) F. J. Steemers, W. Verboom, D. N. Reinhoudt, E. B. VanderTol and J. W. Verhoeven, *J. Am. Chem. Soc*., **1995**, *117*, 9408–9414; (b) H. Xu, H. L. Wang, X. H. Zhu, K. Yin, G. Y. Zhong, X. Y. Hou, W. Huang, *J. Phys. Chem. B*, **2006**, *110*, 3023–3029.

[29] a) G. Bobba, Y. Bretonnière, J.-C. Frias, D. Parker, *Org. Biomol. Chem*. **2003**, *1*, 1870-1872; b) G. Bobba, R. S. Dickins, J. A. G. Williams, C. F. G. C. Geraldes, *et al., J. Chem. Soc. Perkin Trans.*, **2001**, *2*, 1729-1737.

[30] a) V. Divya, M. L. P. Reddy, R. Pavithran, *Dalton Trans.* **2013**, *42*, 15249–15262; b) V. Divya, V. Sankar, K. G. Raghu, M. L. P. Reddy, *Dalton Trans*. **2013**, *42*, 12317-12323; c) D. B. Ambili Raj, S. Biju, M. L. P. Reddy, *Inorg. Chem.* **2008**, *47*, 8091−8100.

[31] a) J. Yu, L. Zhou, H. Zhang, Y. Zheng, H. Li, R. Deng, Z. Peng, Z. Li, *Inorg. Chem.* **2005**, *44*, 1611-1618; b) J. Li, H. Li, P. Yan, P. Chen, G. Hou, G. Li, *Inorg. Chem.* **2012**, *51*, 5050−5057; c) J. Sun, B. Song, Z. Ye, J. Yuan, *Inorg. Chem.* **2015**, *54*, 11660−11668; d) J. Shi, Y. Hou, W. Chu, X. Shi, H. Gu, B. Wang, Z. Sun, *Inorg. Chem.* **2013**, *52*, 5013-5022.

[32] a) M. J. Frisch, G. W. Trucks, H. B. Schlegel, *et al., Gaussian 09, Revision D.01*, Gaussian, Inc., Wallingford, CT, **2009**; b) L. Yang, X. Wang, G. Zhang, X. Chen, G. Zhang, J. Jiang, *Nanoscale*, **2016**, *8*, 17422–17426.

[33] B. Rajamouli, V. Sivakumar, *New J. Chem*. **2017**, *41*, 1017-1027.

[34] a) W. D. Horrocks, Jr. D. R. Sudnick, *J. Am. Chem. Soc.* **1979**, *101*, 334-340; b) A. Beeby, I. M. Clarkson, R. S. Dickins, S. Faulkner, D. Parker, L. Royle, A. S. de Sousa, J. A. G. Williams, M. Woods, *J. Chem. Soc., Perkin Trans. 2*, **1999**, 493-504.

[35] G. R. Choppin, D. R. Peterman, *Coord. Chem. Rev.* **1998**, *174*, 283–299.

[36] D. Costa, H. D. Burrows, M. da Gracüa, *Langmuir*, **2005**, *21*, 10492–10496.

[37] a) K. Binnemans, *Chem. Rev*. **2009**, *109*, 4283; b) X. Zhang, Y. Jiao, X. Jing, H. Wu, G. He, C. Duan, *Dalton Trans*. **2011**, *40*, 2522-2527; c) Y. Lu, B. Yan, *Chem. Commun*. **2014**, *50*, 13323-13326.

[38] (*a*) T. Gunnlaugsson, A. Harte, J. P. Leonard, M. Nieuwenhuyzen, *Supramol. Chem.,* **2003**, *15*, 505; (*b*) T. Gunnlaugsson, A. Harte, J. P. Leonard, M. Nieuwenhuyzen, *Chem. Commun*., **2002**, 2134-2135.

[39] a) S. J. A. Pope, B. P. Burton-Pye, R. Berridge, T. Khan, P. J. Skabara, S. Faulkner, *Dalton Trans*. **2006**, 2907-2912; b) R. S. Dickins, T. Gunnlaugsson, D. Parker, R. D. Peacock, *Chem. Commun*. **1998**, 1643-1650; c) C. Li, W.-T. Wong, *Chem. Commun*. **2002**, 2034-2035.

[40] a) P. A. Gale, *Acc. Chem. Res*., **2006**, *39*, 465-475; P. A. Gale, *Chem. Commun*. **2005**, 3761-3772; b) T. Gunnlaugsson, P. E. Kruger, P. Jensen, J. Tierney, H. D. P. Ali, G. M. Hussey, *J. Org. Chem*. **2005**, *70*, 10875-10878.

[41] a) A. T. Wright, E. V. Anslyn, *Chem. Soc. Rev*. **2006**, *35*, 14-28; b) S. L. Wiskur, H. Ait-Haddou, J. J. Lavigne, E. V. Anslyn, *Acc. Chem. Res*. **2001**, *34*, 963-972.

[42] a) T. M. Kelly, A. B. Tossi, D. J. McConnell, T. C. Strekas, *Nucleic Acids Res*. **1985**, *13*, 6017-6034; b) A. M. Pyle, J. P. Rehamann, R. Meshoyrer, C. V. Kumar, N. J. Turro, J. K. Barton, *J. Am. Chem. Soc*. **1989**, *111*, 3051-3058; c) V. A. Bloomfield, D. M. Crothers, I. Tinocoo Jr, *Physical Chemistry of Nucleic Acids*, Harper & Row, New York, **1974**.

[43] a) A. Wolfe, G. H. Shimer, T. Meehan Jr, *Biochemistry*, **1987**, *26*, 6392-6396; b) A. Pyle, J. K. Barton, S. J. Lippard (Ed.), *Progress in Inorganic Chemistry*, **1990**, *38*, 413-475; c) P. J Dandliker, R. E Holmlin, J. K Barton, *Science*, **1997**, *275*, 1465-1468; d) R. Palchaudhuri, P. J. Hergenrother, *Curr. Opin. Biotechnol*. **2007**, *18*, 497-503.

[44] a) X. Li, Z. Yang, *Chem. Biol. Interact*., **2015**, *232,* 77-84; b) J. R. Lakowicz, *Principles of Fluorescence Spectroscopy*, Springer, New York, 3rd edn, **2006**.

[45] Y.-Q. Wang, H.-M. Zhang, G.-C. Zhang, W.-H. Tao, S.-H. Tang, *J. Lumin.* **2007**, *126*, 211–218.

[46] a) D. Hvasanov, A. F. Mason, D. C. Goldstein, M. Bhadbhade, P. Thordarson, *Org. Biomol. Chem.* **2013**, *11*, 4602-4612; b) P. Laine, F. Bedioui, P. Ochsenbein, V. Marvaud, M. Bonin, E. Amouyal *J. Am. Chem. Soc.* **2002**, *124*, 1364–1377.

[47] L. R. Melby, N. J. Rose, E. Abramson, J. C. Caris, *J. Am. Chem. Soc.* **1964**, *86*, 5117–5125.

[48] M. E. Reichmann, S. A. Rice, C. A. Thomas, P. Doty, *J. Am. Chem. Soc*. **1954**, *76*, 3047–3053.

10.1002/ejic.201701495

WILEY-VCH

Entry for the Table of Contents

FULL PAPER

pH-Responsive Luminescent Europium(III) Probe: A luminescent ternary pH-responsive probe, $[Eu(tta)_3(naptpy)]$ was designed utilizing acid-sensitive β-diketonate for potential anion sensing *via* lanthanide based displacement assay.

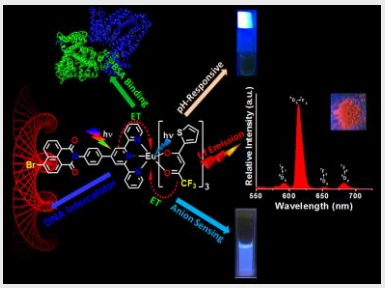

Key Topic*

*Kritika Gupta and Ashis K. Patra**

Page No. – Page No.

A Luminescent pH-Responsive Ternary Eu^{3+} Complex of *β*-diketonate and Terpyridine Derivative as Sensitizing Antenae: Photophysical Aspects, Anion Sensing and Biological Interactions